Japanese Journal of Applied Physics
Vol. 43, No. 2, 2004, pp. 459–466

Temperature Dependence of the Band-Edge Transitions of ZnCdBeSe

Chang-Hsun HSIEH, Ying-Sheng HUANG*, Ching-Hwa HO[1], Kwong-Kau TIONG[2], Martin MUÑOZ[3], Oleg MAKSIMOV[3] and Maria C. TAMARGO[3]

Department of Electronic Engineering, National Taiwan University of Science and Technology, Taipei 106, Taiwan, Republic of China
[1]*Department of Materials Science and Engineering, National Dong Hwa University, Shoufeng, Hualien 974, Taiwan, Republic of China*
[2]*Department of Electrical Engineering, National Taiwan Ocean Univesity, Keelung 202, Taiwan, Republic of China*
[3]*Center for Advanced Technology (CAT) on Photonic Materials and Applications, Center for Analysis of Structures and Interfaces (CASI), Department of Chemistry, City College-CUNY, New York, NY 10031, USA*

(Received May 13, 2003; accepted October 29, 2003; published February 10, 2004)

We have characterized the temperature dependence of band-edge transitions of three $(Zn_{0.38}Cd_{0.62})_{1-x}Be_xSe$ II–VI films with different Be concentrations x by using contactless electroreflectance (CER) and piezoreflectance (PzR) in the temperature range of 15 to 450 K. By a careful comparison of the relative intensity of PzR and CER spectra, the identification of light-hole (lh) and heavy-hole (hh) character of the excitonic transitions of the samples has been accomplished. The temperature dependence analysis yields information on the parameters that describe the temperature variations of the energy (including thermal expansion effects) and broadening parameter of the band edge transitions of ZnCdBeSe. The study shows that Be incorporation can effectively reduce the rate of temperature variation of the energy gap. [DOI: 10.1143/JJAP.43.459]

KEYWORDS: ZnCdBeSe, electroreflectance, piezoreflectance, temperature dependent band gap, broadening parameter

1. Introduction

Recently the growth of II–VI wide-band-gap semiconductor heterostructures has attracted considerable attention due to their novel physical properties and a wide range of applications in optoelectronic devices. The applications include the use of II–VI compound based materials as light sources, in full color displays and for increasing the information density in optical recording. Thin films of ZnCdBeSe II–VI compounds grown on III–V compound substrates are of particular interest in the device applications of light emitting diodes (LEDs) and laser diodes (LDs) of visible and UV spectral region due to their good operation stability in terms of temperature variation and lifetime.[1–3] According to theoretical prediction and subsequent experimental verification, the beryllium containing II–VI compounds had been found to possess an enhanced ability to significantly reduce the defects propagation due to a more prevalence of strong covalent bonding and lattice hardening in the materials.[4,5] The strong covalent bonding in beryllium-based II–VI compounds achieves a considerable lattice hardening which avoids multiplication of defects during the operation of II–VI semiconductor laser devices.[6,7] Up-to-date, in spite of the anticipated advantages of the Be-based II–VI compounds, very little work has been done on the temperature dependence of the near band edge transitions of these materials. The temperature dependence of the energy and broadening of interband electronic transitions can yield important information concerning the physical properties of the materials such as electron (exciton)–phonon interactions, excitonic effects, etc. The practical aspect of this investigation is related to the control of the operating temperature of the laser structure itself. An increase in temperature leads to a red shift of band gaps as well as an increase in the linewidth.

In this article, we report a detailed study of the temperature dependence of the energy and broadening parameter of the near band edge interband transitions of three $(Zn_{0.38}Cd_{0.62})_{1-x}Be_xSe$ films, grown on InP substrates, using contactless electroreflectance (CER) and piezoreflectance (PzR) measurements in the temperature range of 15 to 450 K. The identification of the light-hole (lh) and heavy-hole (hh) character of the excitonic transitions of $(Zn_{0.38}Cd_{0.62})_{1-x}Be_xSe$ samples has been accomplished by comparing the relative intensity of the PzR and CER spectra. Transition energies for the band-to-band excitonic transitions of $(Zn_{0.38}Cd_{0.62})_{1-x}Be_xSe$ are determined by fitting the experimental spectra to a Lorentzian line-shape function. Two factors, namely, the thermal expansion and electron (exciton)–phonon coupling effects contribute to the temperature shift of the transition energy of $(Zn_{0.38}Cd_{0.62})_{1-x}Be_xSe$ compounds. Thermal expansion effect[8,9] can be accounted for and the parameters that describe the temperature variation of energy and broadening function of lh and hh transitions for ZnCdBeSe are evaluated and discussed. Our study shows evidence of reduced temperature variation of the energy gap upon adding beryllium to the ZnCdSe system.

2. Experimental

The schematic of $(Zn_{0.38}Cd_{0.62})_{1-x}Be_xSe$ epilayers grown on InP substrate by molecular beam epitaxy is shown in Fig. 1. Prior to the growth, the InP substrate was deoxidized at 480°C and an InGaAs buffer layer was grown at 450°C for 5 min. in III–V chamber. Then, the sample was transferred in ultra high vacuum to the II–VI chamber. Keeping the substrate temperature at 170°C, a Zn irradiation was performed for 20 s and a ZnCdSe buffer layer was grown for 1 min. After the growth of ZnCdSe buffer layer, the substrate temperature was increased to 250°C and the ZnCdBeSe film was grown for 1 h. The thickness of the film was about 1.0 μm. Three samples (A, B and C) with different Be concentrations were prepared. In order to obtain a reasonable estimate of the Be content of the quarternary ZnCdBeSe system, a test ternary ZnCdSe alloy (sample A) was also grown together with the quaternary system using the same Zn/Cd flux ratio. The composition of the ZnCdSe was then determined from the lattice constant measured by single and double-crystal X-ray diffraction (XRD) using the Cu $K_{\alpha 1}$ radiation. The full width at half maximum (HWHM)

*Corresponding author. E-mail address: ysh@et.ntust.edu.tw

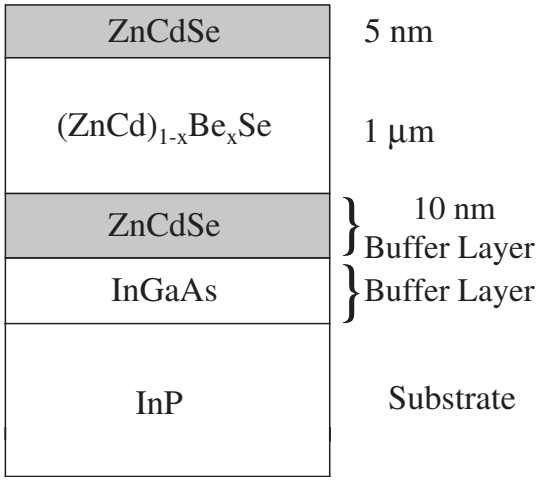

Fig. 1. Schematic for the epitaxial structure of ZnCdBeSe samples.

of the (004) rocking curves of the ZnCdSe sample is rather broad, indicating that the sample is partially strained. The asymmetrical reflection double-crystal X-ray rocking curve (DCXRC) was used to obtain the perpendicular and parallel lattice constants: $a_\perp$ and $a_\parallel$. The bulk lattice constant, a_0, can then be calculated from the equation[10)]

$$a_0 = a_\perp\left[1 - \frac{2\nu}{1+\nu}\frac{a_\perp - a_\parallel}{a_\perp}\right] \quad (1)$$

where ν is Poisson's ratio and a value of $\nu = 0.28$[10)] was used for the present calculation. Then, assuming that Vegard's law is valid for ZnCdSe, the composition of Zn for the sample was calculated. We have used the following values of the lattice constants: $a_{\mathrm{ZnSe}} = 5.6676$ Å[11)] and $a_{\mathrm{CdSe}} = 6.052$ Å[11)] in the calculation. The composition of the ZnCdSe film was also examined by electron probe microanalysis (EPMA). The deviation in the Zn composition between XRD and EPMA is less than 2%. For the as grown quarternary system, we assumed that Be incorporation did not affect the sticking coefficients of Zn and Cd. A similar estimation of the lattice constant parallel to the ternary system was performed. The difference in the lattice constant of ZnCdSe and ZnCdBeSe was then utilized to estimate the Be content. The results are as following: Sample A is $Zn_{0.38}Cd_{0.62}Se$ whose lattice constant is 5.907 Å, and the lattice mismatch to InP is −0.65%, while sample B is $(Zn_{0.38}Cd_{0.62})_{0.93}Be_{0.07}Se$ with a lattice constant 5.842 Å and lattice mismatch of 0.45%. Sample C is $(Zn_{0.38}Cd_{0.62})_{0.89}Be_{0.11}Se$. The lattice constant of sample C is 5.83 Å and the lattice mismatched is 0.63%. It is known that the ratio of $a_\parallel$ to $a_\perp$ can give the strain information directly. The values of $a_\parallel/a_\perp$ of the samples have been checked. The number for sample A is slightly smaller than one ($a_\parallel/a_\perp = 0.996$) while the values for samples B and C are determined to be 1.006 and 1.009 respectively. This might imply a compressive type stress in sample A and the existence of tensile-type stress in samples B and C. These results are further confirmed with the CER and PzR measurements as described in the following section.

The implementation of the CER experiment utilizes a condenser-like system consisting of a front wire grid electrode with a second electrode separated from the first electrode by insulating spacers, which are ∼0.1 mm larger than the sample thickness. The sample is placed in between two capacitor plates such that no direct contact with the front surface of the sample would be made. The probe beam is incident through the front wire grid. Electric field modulation is achieved by applying an ac voltage (∼1 kV peak to peak at 200 Hz) across the electrodes. A 150 W xenon arc lamp filtered by a 0.35 m monochromator provided the monochromatic light. The reflected light was detected by a UV-enhanced silicon photodiode and the dc output of silicon photodiode was maintained constant by a servo mechanism of variable neutral density filter (VNDF). A dual-phase lock-in amplifier was used to measure the detected signals. For temperature dependent measurements, a closed-cycle cryogenic refrigerator equipped with a digital thermometer controller was used for the low-temperature measurements. For the high-temperature experiments, each sample was mounted on one side of a copper finger of an electrical heater, which enabled one to control and stabilize the sample temperature. The temperature dependent measurements were made between 15 and 450 K with a temperature stability of 0.5 K or better. PzR measurements were achieved by sticking each sample with glue on a 0.15 cm thick lead-zirconate-titanate (PZT) piezoelectric transducer driven by a $200\,V_{\mathrm{rms}}$ sinusoidal wave at 200 Hz. The alternating expansion and contraction of the transducer subjects the sample to an alternating strain with a typical rms $\Delta l/l$ value of $\sim 10^{-5}$.

3. Results and Discussion

Figures 2(a) and 2(b) illustrate the CER and PzR spectra of three $(Zn_{0.38}Cd_{0.62})_{1-x}Be_xSe$ samples at 15 K and 300 K, respectively. The experimental data for CER and PzR are shown, respectively, as square and circle curves in Figs. 2(a) and 2(b). These spectra exhibit doublet features near the band edge of $(Zn_{0.38}Cd_{0.62})_{1-x}Be_xSe$. These features are quite similar to those of the excitonic transitions in ZnTe/SLSs/GaAs examined by Tu *et al.*[12,13)] The appearance of the doublets has been shown to be an indication of the heavy-hole (hh) and light-hole (lh) related excitonic transitions.[12,13)] The transition features for beryllium containing samples B and C present an energy blue-shift behavior and a broadened line-shape character with respect to the beryllium-free sample A. The broader line-shape for the samples B and C can be attributed in part, to the alloy scattering effects and most likely, in a larger proportion due to the poorer crystalline quality in the beryllium-incorporated samples. The experimental spectra in Fig. 2 was fitted to first derivative Lorentzian line shape (FDLL) function of the form[14–16)]

$$\frac{\Delta R}{R} = \mathrm{Re}\sum_{j=1}^{2} A_j e^{i\Phi_j}(E - E_j + i\Gamma_j)^{-n} \quad (2)$$

where A_j and Φ_j are the amplitude and phase of the line shape, E_j and Γ_j are the energy and broadening parameter of the transitions, and the value of n depends on the origin of the transitions. For the first derivative functional form, $n = 2$ is appropriate for the bound states such as excitons.[15)] The FDLL fits for both CER and PzR spectra clearly show two structures (indicate with arrows) near the band edge of

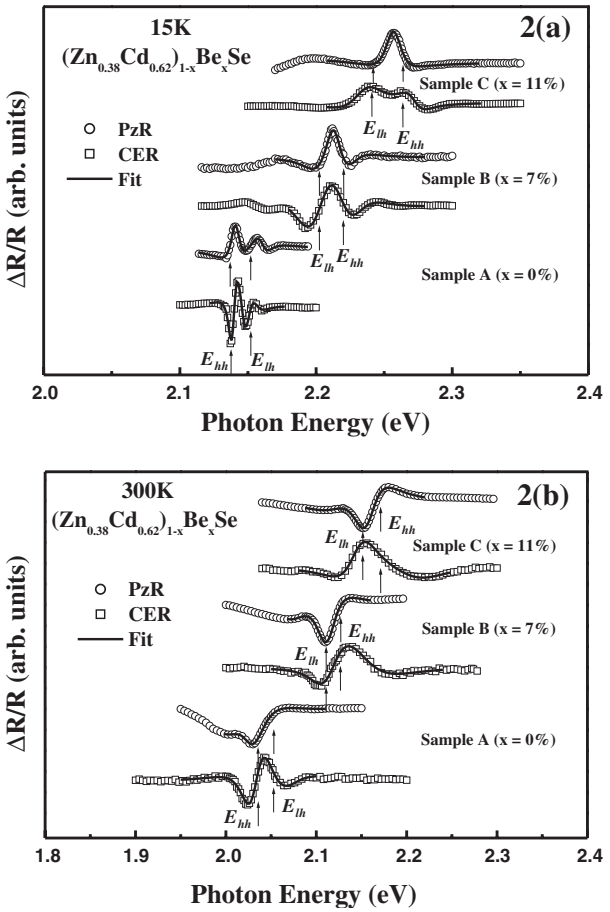

Fig. 2. CER and PzR spectra for three different compositions of ZnCdBeSe samples in spectral range between 1.9 and 2.4 eV at (a) 15 K and (b) 300 K.

$(Zn_{0.38}Cd_{0.62})_{1-x}Be_xSe$. To identify the physical origin of the doublets, we make a spectral comparison of the CER and PzR measurements.

For the PzR measurement under [001]-symmetry coplanar stress, the ratio between the light-hole to electron and heavy-hole to electron transitions under the coplanar piezomodulation has been shown to obey the relation[16,17]

$$K_{PzR} = \frac{(dE_{\rm lh}/dS)}{(dE_{\rm hh}/dS)} = \frac{a(2-\lambda)+b(1+\lambda)}{a(2-\lambda)-b(1+\lambda)}, \qquad (3)$$

The variable S refers to the modulating stress applied to the sample. The parameters a and b represent the hydrostatic and the shear deformation potentials, respectively and $\lambda = -2S_{12}/(S_{11}+S_{12})$, where S_{ij}, $i,j = 1$ or 2, is the elastic compliance constant. For $Zn_{0.38}Cd_{0.62}Se$, the numerical values $S_{11} = 2.33 \times 10^{-3}\,\mathrm{kbar}^{-1}$, $S_{12} = -0.884 \times 10^{-3}\,\mathrm{kbar}^{-1}$, $a = -4.19\,\mathrm{eV}$ and $b = -0.95\,\mathrm{eV}$, are deduced.[11,18] These values are assumed for the present Be-incorporated samples as the concentration of Be is small. The ratio of K_{PzR} is then evaluated to be about 4.6 from eq. (3). This result indicates that the transition of light hole is more sensitive than that of heavy hole under the [001]-symmetry coplanar piezomodulation. The CER spectrum of the same sample, in which the relative intensity of the lh and hh transitions is insensitive to strain, has been used as a reference. The ratio $(dE_{\rm lh}/dS)/(dE_{\rm hh}/dS)$ is relative to $(I_{\rm lh}/I_{\rm hh})_{\rm PzR}$ in the PzR spectra and $(I_{\rm lh}/I_{\rm hh})_{\rm CER}$ in the CER spectra. In the strain-insensitive CER spectra the modulation coefficient is the same for all transitions, so that the ratio $(I_{\rm lh}/I_{\rm hh})_{\rm PzR}/(I_{\rm lh}/I_{\rm hh})_{\rm CER}$ gives that ratio of the piezomodulation coefficients of the lh and hh transitions. From the PzR measurements for the beryllium free sample A, the enlarged lh feature appeared at the higher energy side with respect to the hh feature indicating the presence of a compressive-type stress in the sample. The $K_{\rm PzR}$ is determined to be 1.5 and 2.6 at 15 and 300 K, respectively. However, in samples B and C, the enlarged lh feature appeared at the lower energy side, the $K_{\rm PzR}$ is determined to be 1.8 (2.1) and 1.2 (1.5), respectively, for samples B and C at 15 K (300 K). The lower energy value of the lh transition for ZnCdBeSe sample provides an evidence that tensile-type stress exists in the ZnCdBeSe epitaxial layers of samples B and C. The identified transition features are denoted as $E_{\rm lh}$ and $E_{\rm hh}$ and indicated with arrows in Fig. 2. The difference between the experimentally deduced values of $K_{\rm PzR}$ and that of the theoretical calculation might be attributed to the partial relaxation of the samples. Further evident points to the partial relaxation of the samples can be derived form the evaluation of the strain induced splitting of the heavy hole and light hole transitions defined as $\Delta E \equiv E_{\rm hh} - E_{\rm lh}$. A calculation for the fully strained sample led to $\Delta E = -28\,\mathrm{meV}$, 20 meV and 29 meV, respectively, for samples A, B and C at 300 K. Our experimental values for ΔE at 300 K were determined to be $-17 \pm 4\,\mathrm{meV}$, $16 \pm 4\,\mathrm{meV}$ and $20 \pm 4\,\mathrm{meV}$ respectively, for the three samples. The smaller measured ΔE values is an indication of partial relaxation of the strained layers. Further evidence of partial relaxation also showed up in the low temperature measurement at 15 K, which yielded $\Delta E = -15 \pm 2\,\mathrm{meV}$, $18 \pm 2\,\mathrm{meV}$ and $22 \pm 2\,\mathrm{meV}$ respectively for samples A, B and C. The similarity of ΔE at 300 K and 15 K is contrary to what one generally expects for a strained layer. The thermal expansion coefficients at room temperature for InP,[18] ZnSe,[11] wurtzite CdSe[19] and BeSe[19] are found to be $4.75 \times 10^{-6}\,\mathrm{K}^{-1}$, $7.7 \times 10^{-6}\,\mathrm{K}^{-1}$, $7.3 \times 10^{-6}\,\mathrm{K}^{-1}$, $8.7 \times 10^{-6}\,\mathrm{K}^{-1}$, respectively. The thermal expansion coefficients for $Zn_{0.38}Cd_{0.62}Se$, $(Zn_{0.38}Cd_{0.62})_{0.93}Be_{0.07}Se$ and $(Zn_{0.38}Cd_{0.62})_{0.89}Be_{0.11}Se$ are determined to be $7.45 \times 10^{-6}\,\mathrm{K}^{-1}$, $7.54 \times 10^{-6}\,\mathrm{K}^{-1}$ and $7.59 \times 10^{-6}\,\mathrm{K}^{-1}$, respectively, by linear interpolation of values of the end-point materials. At 15 K, since we can not find any data of expansion coefficient for CdSe and BeSe, we tentatively take the ZnSe value of this parameter for the ZnCdBeSe samples. The values of the expansion coefficients for InP[18] and ZnSe[11] at 15 K are $-0.1 \times 10^{-6}\,\mathrm{K}^{-1}$ and $-0.3 \times 10^{-6}\,\mathrm{K}^{-1}$, respectively. In view of the differences in the linear expansion coefficients at 300 K and 15 K, we should expect to observe some variations of ΔE at the two temperatures due to the additional induced strain. The fact that no appreciable difference in the measured ΔE can be observed may indicate the state of partial relaxation of the strained layer. We have also estimated the critical thicknesses of the samples from the elastic constants. The estimated critical thicknesses are about an order smaller than the sample thickness of $\sim 1.0\,\mu\mathrm{m}$. This means that the samples should relax completely. However, our experimental results seem to indicate the existence of residual strain even for sample thickness much larger than the critical thickness. Similar existence of residual stain is also found

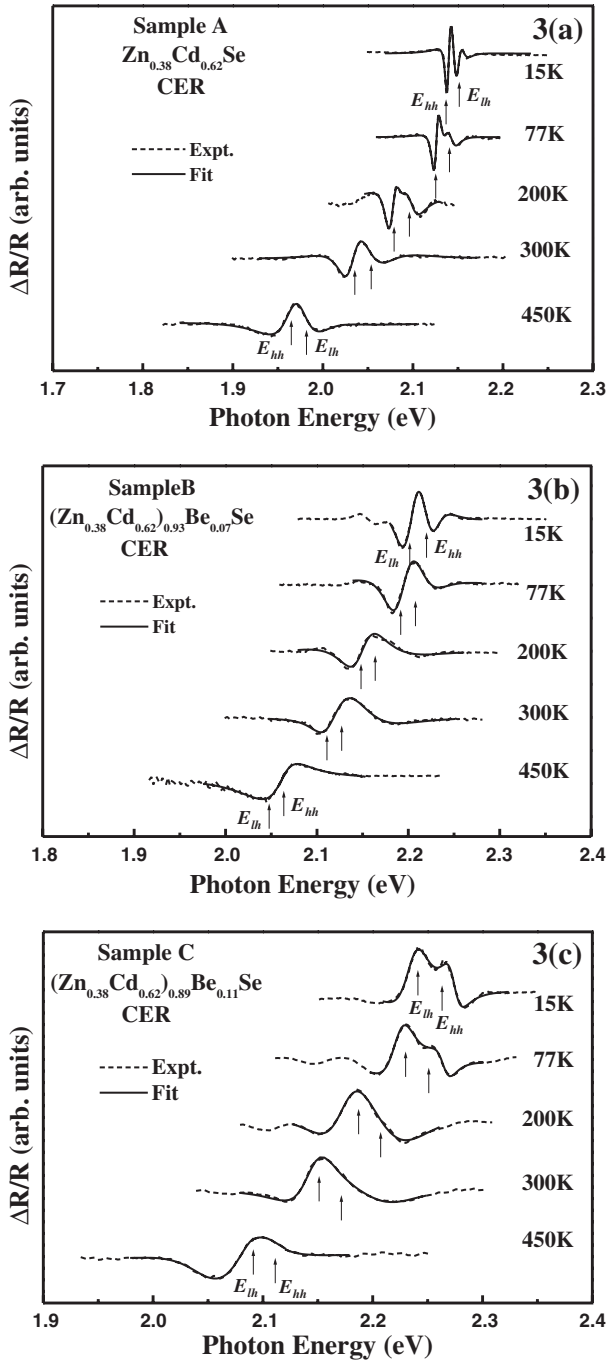

Fig. 3. Experimental CER spectra of (a) $Zn_{0.38}Cd_{0.62}Se$ (Sample A), (b) $(Zn_{0.38}Cd_{0.62})_{0.93}Be_{0.07}Se$ (Sample B), and (c) $(Zn_{0.38}Cd_{0.62})_{0.89}Be_{0.11}Se$ (Sample C) at several temperatures between 15 and 450 K. The dashed lines are the experimental curves and the solid lines are least-squares fits to eq. (2).

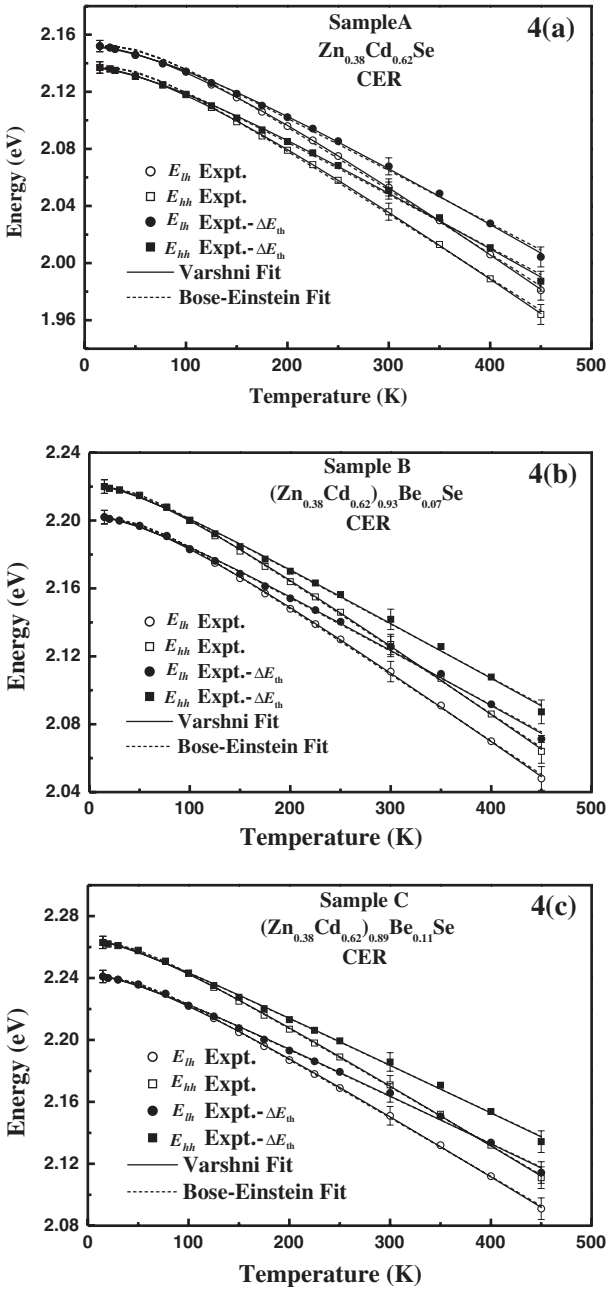

Fig. 4. The temperature variations of light-hole (lh) and heavy-hole (hh) transition energies of (a) $Zn_{0.38}Cd_{0.62}Se$ (Sample A), (b) $(Zn_{0.38}Cd_{0.62})_{0.93}Be_{0.07}Se$ (Sample B), and (c) $(Zn_{0.38}Cd_{0.62})_{0.89}Be_{0.11}Se$ (Sample C) with representative error bars. The solid curves are least-squares fits to the Varshni-type semiempirical relationship and the dashed lines are fitted to the Bose–Einstein-type expression.

for InGaAs films grown on GaAs substrate.[20] The physical origin of this residual strain is not clear and more investigative works should be performed to clarify this point. In addition, a broad feature located at the lower energy side of the low-temperature spectra of samples B and C was observed. This feature is most probably related to some structural defects at the II–VI/III–V interface in samples B and C.

Displayed by dashed curves in Figs. 3(a), 3(b) and 3(c) are, respectively, the experimental CER spectra of samples A, B and C at several temperatures between 15 and 450 K. The solid lines are the fitted spectral data to eq. (2) with $n = 2$, which yield transition energies indicated by arrows. As the general property of most semiconductors, when the temperature is increased, the lh and hh transitions in the CER spectra exhibit an energy red-shift and lineshape broadening characteristics. The broader lineshapes of the transition features are due to the increase of lattice-phonon scattering effects.

Plotted by the open circles and open squares in Figs. 4(a), 4(b) and 4(c) are the temperature variations of the experimental values of E_{lh} and E_{hh}, respectively with the representative error bars for ZnCdBeSe samples A, B and C. The temperature shift of the transition energies contains

Table I. Values of the Varshni-type fitting parameters, which describe the temperature dependence of transition energies of $Zn_{0.38}Cd_{0.62}Se$, $(Zn_{0.38}Cd_{0.62})_{0.93}Be_{0.07}Se$, and $(Zn_{0.38}Cd_{0.62})_{0.89}Be_{0.11}Se$ obtained from the CER experiments. The parameters for ZnSe, $Zn_{0.56}Cd_{0.44}Se$, CdSe, GaAs, InP, and $In_{0.06}Ga_{0.94}As$ are included for comparison.

Material	$E_g^j(0)$ (eV)	α_j (10^{-4} eV/K)	β_j (K)	α'_j (10^{-4} eV/K)	β'_j (K)
$Zn_{0.38}Cd_{0.62}Se$[a]					
E_{hh}	2.138 ± 0.002	5.6 ± 0.2	195 ± 20	4.5 ± 0.2	150 ± 20
E_{lh}	2.153 ± 0.002	5.7 ± 0.2	210 ± 20	4.5 ± 0.2	160 ± 20
$(Zn_{0.38}Cd_{0.62})_{0.93}Be_{0.07}Se$[a]					
E_{lh}	2.203 ± 0.002	4.9 ± 0.2	180 ± 35	3.9 ± 0.2	140 ± 35
E_{hh}	2.221 ± 0.002	5.1 ± 0.2	190 ± 35	3.9 ± 0.2	130 ± 35
$(Zn_{0.38}Cd_{0.62})_{0.89}Be_{0.11}Se$[a]					
E_{lh}	2.242 ± 0.002	4.8 ± 0.2	175 ± 35	3.7 ± 0.2	125 ± 35
E_{hh}	2.264 ± 0.002	4.8 ± 0.2	160 ± 35	3.7 ± 0.2	115 ± 35
ZnSe[b]	2.800 ± 0.005	7.3 ± 0.4	295 ± 35	5.0 ± 4	206 ± 35
$Zn_{0.56}Cd_{0.44}Se$[b]	2.272 ± 0.004	6.1 ± 0.5	206 ± 35	4.5 ± 0.5	153 ± 45
CdSe[c]	1.834 (3)	4.24 (20)	118 (40)		
GaAs[d]	1.512 ± 0.005	5.1 ± 0.5	190 ± 82		
InP[e]	1.432 ± 0.007	4.1 ± 0.3	136 ± 60		
$In_{0.06}Ga_{0.94}As$[f]	1.420 ± 0.005	4.8 ± 0.4	200 ± 50	2.5 ± 0.4	140 ± 40

a) Present work.
b) ref. 9.
c) ref. 22. The numbers in parentheses are error margins in units of the last significant digit.
d) ref. 23.
e) ref. 24.
f) ref. 8.

contributions from both thermal expansion and electron (exciton)–phonon coupling effects. To obtain the parameters directly related to the latter contribution, it is necessary to eliminate the contribution of the former. The energy shift $\Delta E_{th}(T)$ due to thermal expansion can be written as[8,9]

$$\Delta E_{th}(T) = 3a \int_0^T \alpha(T')dT' \tag{4}$$

where a is the interband hydrostatic deformation potential and $\alpha(T)$ is the temperature-dependent linear-expansion coefficient. For the ZnSe binary compound, the value of a is -5.4 eV and $\alpha(T)$ can be deduced from Ref. 11. For $Zn_{0.38}Cd_{0.62}Se$, a value of $a = -4.2$ eV can be obtained from a linear interpolation between the hydrostatic pressure coefficient of ZnSe and the lowest-lying exciton (A exciton) of wurzite CdSe.[11] Since we found no data for $\alpha(T)$ for CdSe and BeSe, we tentatively take the ZnSe value of this parameter for this II–VI ZnCdBeSe alloy system. The energy terms, which are relevant to the electron (exciton)–phonon scattering influence can be expressed as $E_{lh} - \Delta E_{th}(T)$ and $E_{hh} - \Delta E_{th}(T)$, and illustrated in Figs. 4(a), 4(b) and 4(c) as solid circles and squares, respectively. The transitions energies contain contributions from the thermal expansion and electron–phonon interaction, and can be fitted to the Varshni semiempirical relationship[21]

$$E_j(T) = E_j(0) - \frac{\alpha_j T^2}{(\beta_j + T)} \tag{5a}$$

Here, $E_j(0)$ is the energy at 0 K; α_j and β_j are constants, and j refers to lh or hh. The constant α_j is related to the electron (exciton)–phonon interaction and β_j is closely related to the Debye temperature.[21] If we remove the thermal expansion contribution from $E_g^j(T)$, the Varshni-type relation can be written as[8,9]

$$E_g^j(T) - \Delta E_{th}(T) = E_g^j(0) - \frac{\alpha'_j T^2}{(\beta'_j + T)} \tag{5b}$$

where the primed parameters are defined similarly to the unprimed counterparts in eq. (5a). The temperature dependent energy values of $E_{hh} - \Delta E_{th}(T)$ and $E_{lh} - \Delta E_{th}(T)$ are least-square fits to the eq. (5b) and indicated as solid curves in Fig. 4. The values obtained for $E_j(0)$, α_j, α'_j, β_j and β'_j are listed in Table I together with the fitted parameters for the direct gaps of ZnSe,[9] $Zn_{0.56}Cd_{0.44}Se$,[9] CdSe,,[22] GaAs,[23] InP,[24] and $In_{0.06}Ga_{0.94}As$[8] given for comparison purpose. The nearly equal value of α'_j and that of β'_j for samples A, B, and C, respectively, in Table I indicates that the transitions of lh and hh have almost identical temperature dependence as illustrated in the Fig. 4.

The temperature dependence of excitonic transitions of the ZnCdBeSe II–VI compounds can also be analyzed by a Bose–Einstein type expression of the form[8,9]

$$E_j(T) = E_j(0) - \frac{2a_{jB}}{\left[\exp\left(\frac{\Theta_{jB}}{T}\right) - 1\right]}, \tag{6a}$$

$$E_j(T) - \Delta E_{th}(T) = E_j(0) - \frac{2a'_{jB}}{\left[\exp\left(\frac{\Theta'_{jB}}{T}\right) - 1\right]} \tag{6b}$$

where $E_j(0)$ is the energy value at 0 K, a_{jB} represents the strength of average electron–phonon interaction, and Θ_{jB} corresponds to the average phonon temperature and the index j refers to lh or hh interaction. The primed parameters in eq. (6b) are defined similarly to the unprimed terms in eq. (6a) with the contribution from thermal expansion effect

Table II. Values of the Bose–Einstein-type fitting parameters, which describe the temperature dependence of the transition energies of $Zn_{0.38}Cd_{0.62}Se$, $(Zn_{0.38}Cd_{0.62})_{0.93}Be_{0.07}Se$, and $(Zn_{0.38}Cd_{0.62})_{0.89}Be_{0.11}Se$ obtained from CER experiments. The parameters for ZnSe, $Zn_{0.56}Cd_{0.44}Se$, CdSe, GaAs, InP, and $In_{0.06}Ga_{0.94}As$ are included for comparison.

Material	$E_j(0)$ (eV)	a_{jB} (meV)	Θ_{jB} (K)	a'_{jB} (meV)	Θ'_{jB} (K)
$Zn_{0.38}Cd_{0.62}Se$[a]					
E_{hh}	2.138 ± 0.002	48 ± 4	195 ± 20	36 ± 4	175 ± 20
E_{lh}	2.153 ± 0.002	50 ± 4	205 ± 20	38 ± 4	185 ± 20
$(Zn_{0.38}Cd_{0.62})_{0.93}Be_{0.07}Se$[a]					
E_{lh}	2.203 ± 0.002	46 ± 4	205 ± 30	34 ± 4	185 ± 30
E_{hh}	2.221 ± 0.002	45 ± 4	200 ± 30	33 ± 4	175 ± 30
$(Zn_{0.38}Cd_{0.62})_{0.89}Be_{0.11}Se$[a]					
E_{lh}	2.242 ± 0.002	45 ± 4	205 ± 30	33 ± 4	185 ± 30
E_{hh}	2.264 ± 0.002	44 ± 4	200 ± 30	32 ± 4	175 ± 30
ZnSe[b]	2.800 ± 0.005	73 ± 4	260 ± 10	47 ± 4	220 ± 10
$Zn_{0.56}Cd_{0.44}Se$[b]	2.267 ± 0.004	62 ± 4	236 ± 10	43 ± 4	201 ± 10
CdSe[c]	1.830(5)	36(5)	179(40)		
GaAs[d]	1.512 ± 0.005	57 ± 29	240 ± 102		
InP[e]	1.423 ± 0.01	51 ± 2	259 ± 10		
$In_{0.06}Ga_{0.94}As$[f]	1.420 ± 0.005	44 ± 9	203 ± 45	33 ± 7	280 ± 45

a) Present work.
b) ref. 9.
c) ref. 22. The numbers in parentheses are error margins in units of the last significant digit.
d) ref. 25.
e) ref. 24.
f) ref. 8.

eliminated. The dashed lines shown in Figs. 4(a)–4(c) are the least-squares fits of the relevant energy terms to eq. (5a) or (5b). The obtained values of the fitting parameters are listed in Table II. For comparison, the parameters for the direct gaps of ZnSe,[9] $Zn_{0.56}Cd_{0.44}Se$,[9] CdSe,[22] GaAs,[25] InP,[24] and $In_{0.06}Ga_{0.94}As$[8] are also included. The temperature variations of the excitonic transition energies are dominated by lattice constant variations and the interactions with relevant acoustic and optical phonons. The parameters a'_{jB} and Θ'_{jB} in eq. (6b) are related to α'_j of eq. (5b) by taking the high temperature limit of both expressions. This yields relationship of $\alpha'_j \approx 2a'_{jB}/\Theta'_{jB}$. Comparison of Table I and II shows that within error limits this relationship is satisfied.

The experimental values of the temperature dependence of the linewidth $\Gamma^j(T)$ [half width at half maximum (HWHM)] of the excitonic features for the three ZnCdBeSe Samples, as obtained from the line-shape fits, are displayed in Figs. 5(a), 5(b) and 5(c), respectively. The open and solid circles are the data points of lh and hh transitions and the solid lines are least-square fits to an expression responsible for the temperature dependence of the linewidth of the direct gap for zinc-blende-type semiconductors of the form[26]

$$\Gamma^j(T) = \Gamma^j(0) + \gamma^j_{AC}T + \frac{\Gamma^j_{LO}}{\left[\exp\left(\frac{\Theta^j_{LO}}{T}\right) - 1\right]} \qquad (7)$$

In eq. (7), the index j refers to either lh or hh interactions. The first term of eq. (7) is due to intrinsic effects (electron-electron interaction, impurity, dislocation, and alloy scattering) at $T = 0\,K$, while the second term corresponds to lifetime broadening due to the electron (exciton)–acoustical phonon interaction, where γ^j_{AC} is the acoustical phonon coupling constant. The third term is caused by the electron (exciton)–LO phonon (Fröhlich) interaction. The quantity Γ^j_{LO} represents the strength of the electron (exciton)–LO phonon coupling while Θ^j_{LO} is the LO phonon temperature. As shown in Figs. 5(a)–5(c), as the temperature is raised, the linewidth first increases from its zero-temperature value because of acoustical phonon scattering. Above about 50 K the LO phonon contribution becomes important and eventually dominates the linewidth broadening. In this article, we treat the four terms $\Gamma^j(0)$, γ^j_{AC}, Γ^j_{LO} and Θ^j_{LO} as fitting parameters. Least-squares fits to eq. (6) yields the solid lines as illustrated in Figs. 5(a)–5(c) and the obtained values of $\Gamma^j(0)$ and Γ^j_{LO} as well as the numbers for γ^j_{AC} and Θ^j_{LO} are listed in Table III. For comparison, the values of Γ_{LO} (in terms of HWHM) for ZnSe,[9,26,27] $Zn_{0.56}Cd_{0.44}Se$,[9] CdSe (A exciton),[22] GaAs,[28] $In_{0.06}Ga_{0.94}As$,[8] InP,[29] and GaN[30,31] from other works are also included in Table III. The values of $\Gamma^j(0)$ for the beryllium containing samples are much larger than those of beryllium free sample due mainly to the poorer crystalline quality of the Be-incorporated samples. In fact it is not easy to grow high-quality Be-related II–VI quaternaries.

In general, temperature variations of the energy gap are due to both lattice constant variations and interactions with relevant acoustic and optical phonons. According with existing theory[25,32–34] this leads to a value of $\Theta_{jB}(\Theta'_{jB})$ significantly small than Θ^j_{LO}. From Tables I and II, it can be seen that our observations agree well with this theoretical consideration. Figures 4(a), 4(b), and 4(c) show linearizing of the energy gap as the temperature is raised above $\sim$200 K. Least-square fits by a straight line in this region yields temperature coefficient of the energy shift for either lh or hh interactions (with thermal expansion eliminated) to be

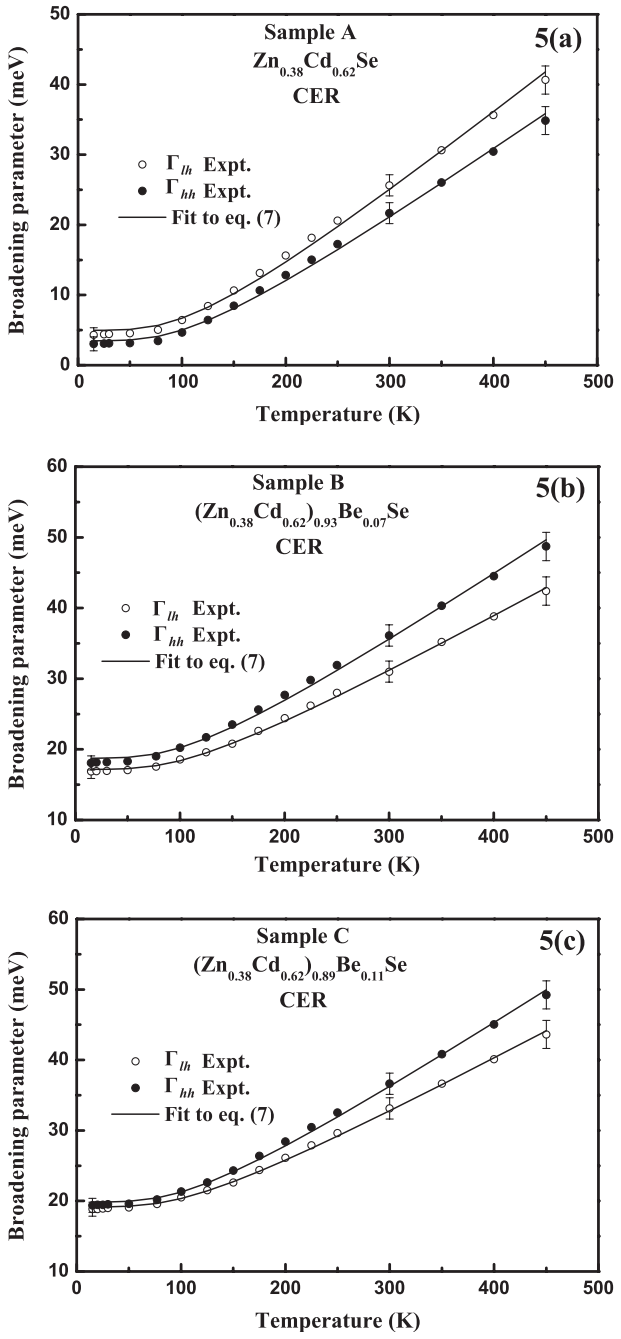

Fig. 5. Experimental variation of the broadening parameter (HWHM) for the direct excitonic transitions of (a) $Zn_{0.38}Cd_{0.62}Se$ (Sample A), (b) $(Zn_{0.38}Cd_{0.62})_{0.93}Be_{0.07}Se$ (Sample B), and (c) $(Zn_{0.38}Cd_{0.62})_{0.89}Be_{0.11}Se$ (Sample C) with representative error bars. The open and solid circles are respectively the experimental values of lh and hh transitions, respectively, and the solid lines are least-square fits to eq. (7).

-3.9×10^{-4} eV/K for sample A, -3.3×10^{-4} eV/K for sample B and -3.1×10^{-4} eV/K for sample C. By taking high temperature limits of either eqs. (5b) or (6b), we can correlate these values to that of α'_j or $\alpha'_{j\mathrm{B}}$ as given in Tables I and II, respectively. These numbers also indicate that the addition of Be reduces the rate of change of the energy gap with temperature for the Be-containing ZnCdSe compounds. This is a desirable feature for the device applications of these compounds. Our fitted values for Γ_{LO} are comparable to that of ZnSe,[9,26,27] CdSe[22] and most of the III–V semiconductors[8,28,29] with the exception of GaN.[30,31] It has been shown theoretically that Fröhlich interaction is stronger in the more ionic crystals of II–VI semiconductors than the III–V semiconductors.[26] Our results show no clear trend to that effect and seem to indicate that other factor may contribute to the electron (exciton)–LO phonon coupling constant, Γ_{LO}. In the case of GaN, it may be possible that a larger deformation potential interaction may contribute a significant proportion to Γ_{LO} in addition to the Fröhlich interaction.[30,31] The ionicity dependence of Fröhlich interaction requires further consideration and more work needs to be done in this area.

Table III. Values of the parameters that describe the temperature dependence of Γ (HWHM) for the energy gaps of $Zn_{0.38}Cd_{0.62}Se$, $(Zn_{0.38}Cd_{0.62})_{0.93}Be_{0.07}Se$, and $(Zn_{0.38}Cd_{0.62})_{0.89}Be_{0.11}Se$ obtained from the CER experiments. The relevant parameters for ZnSe, $Zn_{0.56}Cd_{0.44}Se$, CdSe, GaAs, InP, $In_{0.06}Ga_{0.94}As$ and GaN are also included for comparison.

Material	$\Gamma^j(0)$ (meV)	Γ_{LO} (meV)	Θ_{LO} (K)	γ_{AC} (μeV/K)
$Zn_{0.38}Cd_{0.62}Se$[a]				
E_{hh}	3 ± 2	33 ± 8	320 ± 100	2 ± 1
E_{lh}	4 ± 2	35 ± 8	310 ± 100	2 ± 1
$(Zn_{0.38}Cd_{0.62})_{0.93}Be_{0.07}Se$[a]				
E_{lh}	17 ± 2	25 ± 8	330 ± 100	2 ± 1
E_{hh}	18 ± 2	32 ± 8	335 ± 100	2 ± 1
$(Zn_{0.38}Cd_{0.62})_{0.89}Be_{0.11}Se$[a]				
E_{lh}	19 ± 2	26 ± 8	345 ± 100	2 ± 1
E_{hh}	20 ± 2	31 ± 8	350 ± 100	2 ± 1
ZnSe	6.5 ± 2.5[b]	24 ± 8[b] 30 ± 7[d] 30[e]	360[b),c)]	2.0[b),c)]
$Zn_{0.56}Cd_{0.44}Se$[b]	6.0 ± 2.0	17 ± 6	334[c)]	1.1[c)]
CdSe[f)]	2.3(3)	23(1)	300[c)]	
GaAs[g)]		23 ± 1.5	417[c)]	
$In_{0.06}Ga_{0.94}As$[h)]	7.5 ± 0.5	23 ± 6	370 ± 122	
InP[i)]	1.5 ± 0.5	31 ± 3.0	496[c)]	
GaN	10[j)] 2.4[k)]	375[j)] 390[k)]	1065[c)] 1065[c)]	15 16

a) Present work.
b) ref. 9.
c) Parameter fixed.
d) ref. 26.
e) ref. 27.
f) ref. 22. The numbers in parentheses are error margins in units of last significant digit.
g) ref. 28.
h) ref. 8.
i) ref. 29. Excitonic transition.
j) ref. 30.
k) ref. 31.

4. Summary

In summary, the temperature dependence of band-edge transitions of ZnCdBeSe II–VI compounds with different Be concentration was studied using contactless electroreflectance (CER) in the temperature range of 15 to 450 K. The experimental results of CER spectra for beryllium containing samples demonstrate an energy blue-shift behavior and a broadened lineshape character with respect to the ZnCdSe specimen. Strain modulated piezoreflectance (PzR) measurements were utilized to facilitate the identification of the

light-hole (lh) and heavy-hole (hh) excitonic transitions of the ZnCdBeSe samples. The enhanced lh feature with lower energy in the PzR spectrum provides conclusive evidence that tensile-type stress existed in the ZnCdBeSe epilaxial layers. The temperature variations of transition energies are analyzed by both the Varshni- and Bose–Einstein-type expressions, which take into consideration the contribution of thermal expansion. The parameters extracted from both expressions are found to agree reasonably well by extending into the high temperature regime. In addition, our analysis shows evidence of a reduced energy shift due to temperature variations by incorporating beryllium into the ZnCdSe compound.

Acknowledgements

The authors C. H. Hsieh and Y. S. Huang acknowledge the support of the National Science Council of the Republic of China under Project No. NSC91-2215-E-011-002. Authors C. H. Ho and K. K. Tiong acknowledge the supports of National Science Council under Project Nos. NSC91-2215-E-259-004 and NSC91-2112-M-019-003. M. Muñoz, O. Maksimov, and M. C. Tamargo acknowledge the partial support from the NSF IGERT grant number DGE9972892.

1) F. Fisher, G. Landwehr, Th. Litz, H. J. Lugauer, U. Zehnder, Th. Gerhard, W. Ossau and A. Waag: J. Cryst. Growth **175/176** (1997) 532.
2) T. B. Ng, C. C. Chu, J. Han, G. C. Hua, R. L. Gunshor, E. Ho, E. L. Warlick, L. A. Kolodziejski and A. V. Nurmikko: J. Cryst. Growth **175/176** (1997) 552.
3) F. Vigué, E. Tournié and J. P. Faurie: Appl. Phys. Lett. **76** (2000) 242.
4) A. Waag, F. Fischer, K. Schüll, T. Baron, H. J. Lugauer, Th. Litz, U. Zehnder, W. Ossau, T. Gerhard, M. Keim, G. Reuscher and G. Landwehr: Appl. Phys. Lett. **70** (1997) 280.
5) J. Y. Zhang, D. Z. Shen, X. W. Fan, B. J. Yang and Z. H. Zheng: J. Cryst. Growth **214/215** (2000) 100.
6) A. Muñoz, P. Rodríguez-Hernández and A. Mujica: Phys. Status Solidi B **198** (1996) 439.
7) A. Waag, F. Fischer, H. J. Lugauer, Th. Litz, J. Laubender, U. Lunz, U. Zehnder, W. Ossau, T. Gerhardt, M. Möller and G. Landwehr: J. Appl. Phys. **80** (1996) 792.
8) Z. Hang, D. Yan, F. H. Pollak, G. D. Pettit and J. M. Woodall: Phys. Rev. B **44** (1991) 10546.
9) L. Malikova, W. Krystek, F. H. Pollak, N. Dai, A. Cavus and M. C. Tamargo: Phys. Rev. B **54** (1996) 1819.
10) S. P. Guo, Y. Luo, W. Lin, O. Maksimov, M. C. Tamargo, I. Kuskovsky, V. Tian and G. Neumark: J. Cryst. Growth **208** (2000) 205.
11) *Semiconductors, Physics of II–VI and I–VII Compounds, Semimagnetic Semiconductors*, eds. O. Madelung, Landolt-Börnstein (Springer, New York, 1982) New Series, Group III: Crystal and Solid State Physics, Vol. 17, Subvol. b.
12) R. C. Tu, Y. K. Su, H. J. Chen, Y. S. Huang and S. T. Chou: Appl. Phys. Lett. **72** (1998) 3184.
13) R. C. Tu, Y. K. Su, H. J. Chen, Y. S. Huang, S. T. Chou, W. H. Lan and S. L. Tu: J. Appl. Phys. **84** (1998) 2866.
14) D. E. Aspnes: *Handbook on Semiconductors*, ed. by T. S. Moss (North-Holland, New York, 1980) Vol. 2, p. 109.
15) F. H. Pollak and H. Shen: Mater. Sci. Eng. **R10** (1993) 275.
16) F. H. Pollak: *Semiconductor and Semimetals*, ed. T. P. Pearsall (Academic, New York, 1990) Vol. 32, p. 17.
17) H. Mathieu, J. Allégre and B. Gil: Phys. Rev. B **43** (1991) 2218.
18) *Semiconductors, Physics of Group IV Elements and III–V Compounds*, eds. O. Madelung, Landolt-Börnstein (Springer, New York, 1982) New Series, Group III: Crystal and Solid State Physics, Vol. 17, Subvol. a.
19) V. Kumar and B. S. R. Sastry: Cryst. Res. Technol. **36** (2001) 565.
20) J. H. Chen, W. S. Chi, Y. S. Huang, Y. Yin, F. H. Pollak, G. D. Pettit and J. M. Woodall: Semicond. Sci. Technol. **8** (1993) 1420.
21) Y. P. Varshni: Physica (Amsterdam) **34** (1967) 149.
22) S. Logothetidis, M. Cardona, P. Lautenschlager and M. Garriga: Phys. Rev. B **34** (1986) 2458.
23) H. Shen, S. H. Pan, Z. Hang, J. Leng, F. H. Pollak, J. M. Woodall and R. N. Sacks: Appl. Phys. Lett. **53** (1988) 1080.
24) Z. Hang, H. Shen and F. H. Pollak: Solid State Commun. **73** (1990) 15.
25) P. Lautenschlager, M. Garriga, S. Logothetidis and M. Cardona: Phys. Rev. B **35** (1987) 9174.
26) S. Rudin, T. L. Reinecke and B. Segall: Phys. Rev. B **42** (1990) 11218.
27) N. T. Pelekanos, J. Ding, M. Hagerott, A. V. Nurmikko, H. Luo, N. Samarth and J. K. Furdyna: Phys. Rev. B **45** (1992) 6037.
28) H. Qiang, F. H. Pollak, C. M. Sotomayor Torres, W. Leitch, A. H. Kean, M. Stroscio, G. J. Iafrate and K. W. Kim: Appl. Phys. Lett. **61** (1992) 1411.
29) S. Y. Chung, D. Y. Lin, Y. S. Huang and K. K. Tiong: Semicond. Sci. Technol. **11** (1996) 1850.
30) A. J. Fischer, W. Shan, J. J. Song, Y. C. Chang, R. Horning and B. Goldenberg: Appl. Phys. Lett. **71** (1997) 1981.
31) A. J. Fischer, W. Shan, G. H. Park, J. J. Song, D. S. Kim, D. S. Yee, R. Horning and B. Goldenberg: Phys. Rev. B **56** (1997) 1077.
32) C. K. Kim, P. Lautenschlager and M. Cardona: Solid State Commun. **59** (1986) 797.
33) S. Zollner, S. Gopalan and M. Cardona: Solid State Commun. **77** (1991) 485.
34) P. Lautenschlager, M. Garriga, L. Viña and M. Cardona: Phys. Rev. B **36** (1987) 4821.